OPERATIONAL EXPERIENCE AT J-PARC

Hideaki Hotchi*, 1) for J-PARC commissioning team1), 2),
1)Japan Atomic Energy Agency (JAEA), Tokai, Naka, Ibaraki, 319-1195 Japan,
2)High Energy Accelerator Research Organization (KEK), Tsukuba, Ibaraki, 305-0801 Japan

Abstract

The J-PARC is a multi-purpose proton accelerator facility aiming at MW-class output beam power, which consists of a 400-MeV linac, a 3-GeV rapid cycling synchrotron (RCS), a 50-GeV main ring synchrotron (MR) and several experimental facilities (a materials and life science experimental facility; MLF, a hadron experimental hall; HD, and a neutrino beam line to Kamioka; NU). The beam commissioning of the J-PARC began in November 2006, and then the linac and RCS started a user operation for the MLF in December 2008. The current output beam power to the MLF is 120 kW. In this paper, the recent progress and operational experience in the course of our beam power ramp-up scenario such as beam loss control, machine activation and beam availability, especially obtained in the MLF user operation by the linac and RCS will be presented.

INTRODUCTION

The J-PARC is a multi-purpose proton accelerator facility aiming at MW-class output beam power. As shown in Fig. 1, the J-PARC accelerator complex [1] comprises a 400-MeV linac, a 3-GeV rapid cycling synchrotron (RCS), a 50-GeV main ring synchrotron (MR) and several experimental facilities (a materials and life science experimental facility; MLF, a hadron experimental hall; HD, and a neutrino beam line to Kamioka; NU).

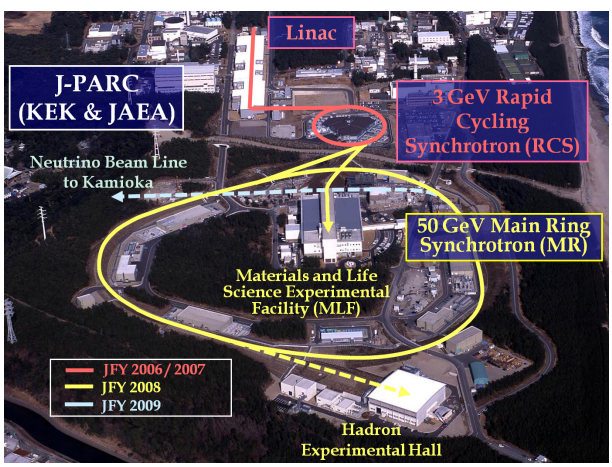

Figure 1: Bird's eye view of the J-PARC.

The linac consists of a H^- ion source, a radio-frequency quadrupole (RFQ), a drift tube linac (DTL) and a separated-type drift tube linac (SDTL). The output energy is 181 MeV and the peak current is 30 mA at present. At full capability in the current configuration, the linac will produce 36 kW output at 181 MeV with 30 mA peak, 0.5 ms long and 56% chopper beam-on duty factor at 25 Hz repetition, which corresponds to 600 kW output at the RCS extraction energy (3 GeV). The upgrade of the front-end system to get 50 mA peak current as well as the installation of an annular coupled structure linac (ACS) for the energy recovery to 400 MeV, which are essential to achieve our final goal of 1 MW output at the RCS, are scheduled for summer maintenance periods in 2012 and 2013.

The linac beam is delivered to the RCS injection point, where it is multi-turn charge-exchange injected with a carbon stripper foil. The RCS accelerates the injected beam up to 3 GeV with 25 Hz repetition. The current injection energy is 181 MeV, for which the RCS will first aim at 300∼600 kW output, and then drive for 1 MW output after upgrading the linac.

The 3-GeV beam from the RCS is mainly transported to the MLF to produce pulsed spallation neutrons and muons. A part of the RCS beam (typically 4 pulses every 3.64 s) is transported to the MR. The MR still accelerates the injected beam to 30 GeV, delivering it to the HD by a slow extraction and to the NU by a fast extraction. The output energy at the MR will be upgraded to 50 GeV in the second phase of the J-PARC project.

The beam commissioning of the J-PARC began in November 2006 and it has well proceeded as planned from the linac to the downstream facilities [2][3]. The linac and RCS started a user operation for the MLF with 4 kW output beam power in December 2008. Via a series of underlying beam studies with such a low intensity beam, the output beam power from the RCS to the MLF was increased to 120 kW in November 2009. Since then, our effort has been focused on a parameter tuning for higher-intensity beams (∼300 kW) including a beam painting injection scheme in the RCS. In this paper, the recent progress and operational experience in the course of our beam power ramp-up scenario such as beam loss control, machine activation and beam availability, especially obtained in the MLF user operation by the linac and RCS will be presented (the status of the MR beam operation is presented in [4] in details).

CURRENT STATUS OF THE LINAC

Fig. 2 shows a typical residual radiation level in the linac, where the top value is a residual radiation level for 4 kW operation measured 6-hour after the beam shutdown, while

* hotchi.hideaki@jaea.go.jp

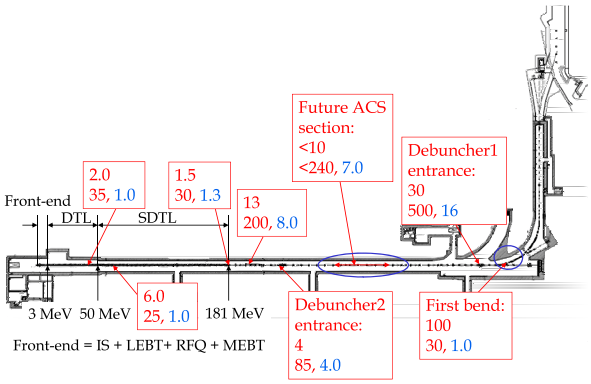

Figure 2: Residual radiation level (μSv/h) in the linac, where the top value is a residual radiation level for 4 kW operation measured 6-hour after the beam shutdown, while the bottom value is for 120 kW operation measured 5-hour after the beam shutdown. In these values, the red one is for the measurement on the surface of the vacuum chamber, while the blue one is at a distance of 30 cm.

the bottom value is for 120 kW operation measured 5-hour after the beam shutdown. In these values, the red one is for the measurement on the surface of the vacuum chamber, while the blue one is at a distance of 30 cm. After startup of a high duty operation for MLF users, we found several significant machine activations [5].

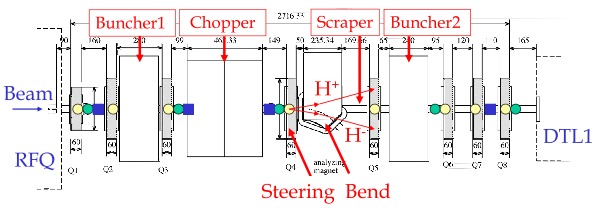

Figure 3: Schematic view of the MEBT.

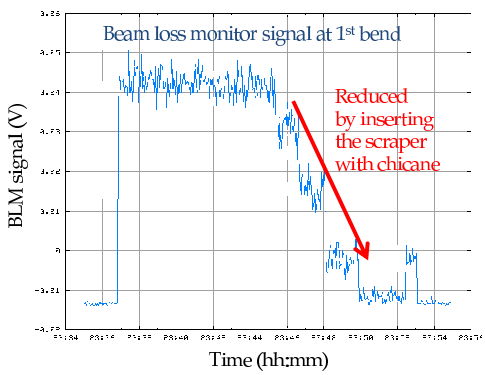

Figure 4: Beam loss monitor signal located near the first bend.

The first one is a residual radiation widely distributed over the future ACS section. One of the possible causes of this particle loss is H^0or H^+ component generated by gas stripping [6]. For this concern, we will add some vacuum pumps in the SDTL and future ACS section in this summer maintenance period (July-September 2010). In the next run cycle (October 2010), we are going to measure this particle loss under the improved vacuum condition.

Another issue was a considerable machine activation at the first bend of the first arc section detected after 4 kW operation, which mainly came from H^+ component accelerated to around the design energy generated by gas stripping in the low energy beam transport line (LEBT) between the ion source and RFQ. For this issue, we tried to remove H^+ component at the medium energy beam transport line (MEBT) between the RFQ and DTL [7]. As shown in Fig. 3, we separated H^+ and H^- with steering and bending magnets, and removed H^+ component with a scraper originally used for chopping. As shown in Fig. 4, the beam loss was reduced to negligible level in this way. Now we use this scheme for routine operation, and the corresponding residual radiation level is significantly reduced to 30 μSv/h on the surface for the current 120 kW routine operation.

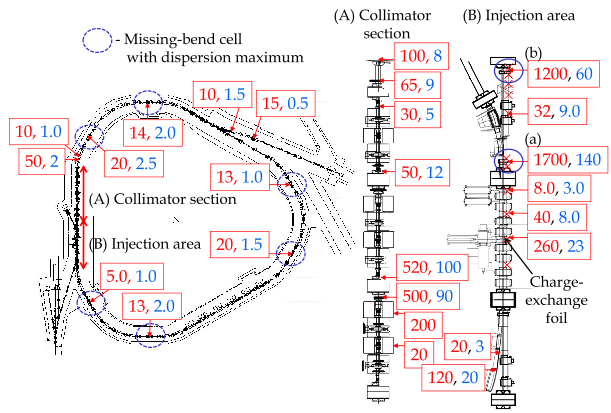

Figure 5: Residual radiation level (μSv/h) in the RCS measured 5-hour after the beam shutdown of 120 kW operation, where the red one is for the measurement on the vacuum chamber surface, while the blue one is at a distance of 30 cm.

CURRENT STATUS OF THE RCS

Fig. 5 shows a typical residual radiation level in the RCS detected 5-hour after the beam shutdown of 120 kW operation. The intensity loss at the RCS for the current 120 kW operation is now 1% level. Most of the beam losses are well localized on the ring collimator, and the residual radiation level in the collimator area is still kept at less than 100 μSv/h at a distance of 30 cm. But small part of them makes some machine activations as unlocalized beam loss [5].

The first one is a machine activation detected downstream of the charge-exchange foil in the injection section, where the highest residual radiation level is 1$\sim$2 mSv/h on the chamber surface. In the RCS, multi-turn charge-exchange injection with a carbon foil is adopted. In this way the beam hits the foil many times during injection period. Fig. 6 shows beam loss monitor signals measured at the two highly activated points (a) and (b) in Fig. 5 as a

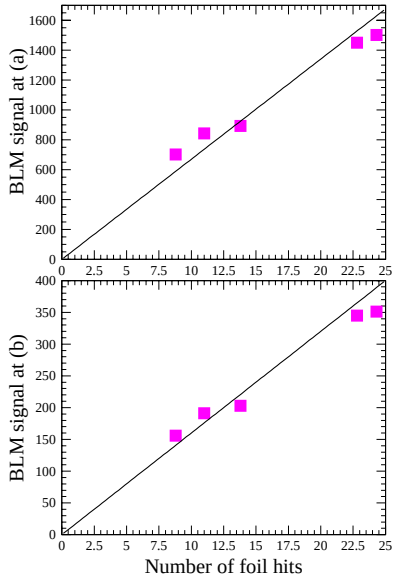

Figure 6: Beam loss monitor signals located at (a) and (b) in Fig 5 as a function of the average number of the foil hits during injection period.

function of the average number of the foil hits during injection period. In this measurement, the number of the foil hits was adjusted by combination of the foil position and the transverse painting. As shown in the figure, the detected beam loss monitor signals are proportional to the number of the foil hits, which indicate that the high residual radiations come from a large angle event from foil scattering. The number of the foil hits in the current 120 kW routine operation is 8.8. The current foil with 110 mm (horizontal)×40 mm (vertical) dimension, which was prepared for the day-1 of the beam commissioning, is too large compared with the actual size of the injection beam (6 mm×6 mm). In order to reduce the foil hitting probability, we will install a new foil with a smaller size in vertical (110 mm ×15 mm) matched to the injection beam size in this summer maintenance period. If using such a small foil, the number of the foil hits can be reduced to 4.7, and the corresponding residual radiations should be half of the current level.

Another one is a machine activation at the arc section with dispersion maximum (6 m). This particle loss takes place at the middle of the acceleration process and is very sensitive for the tune variation during acceleration process and the longitudinal beam profile. Such a feature implies that the beam loss comes from the chromatic tune spread. Now in the RCS the chromatic correction is performed at injection with DC power supplies. Therefore the chromaticity gradually recovers as accelerated. For this concern, we plan to introduce AC power supplies for chromatic correction sextupoles in this summer maintenance period. Another possible cause of this particle loss is a leakage from a distorted rf bucket due to the beam loading effect. In the next run cycle (October 2010), we will try to minimize this particle loss by optimizing the chromatic correction and the tune variation during the acceleration process

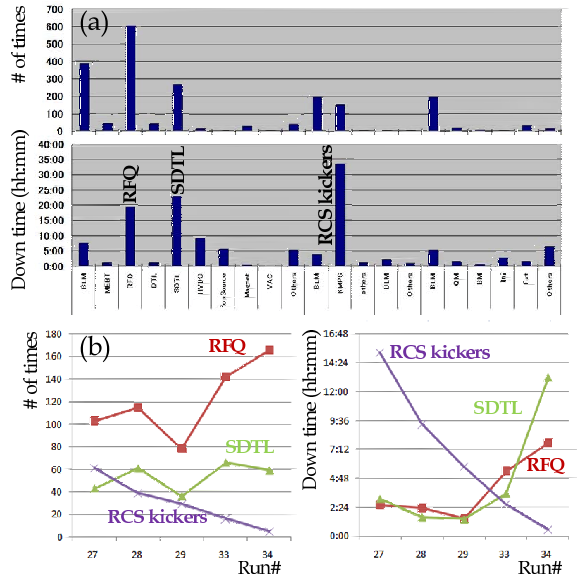

Figure 7: Beam fault statistics for the MLF user operation in the last five run cycles.

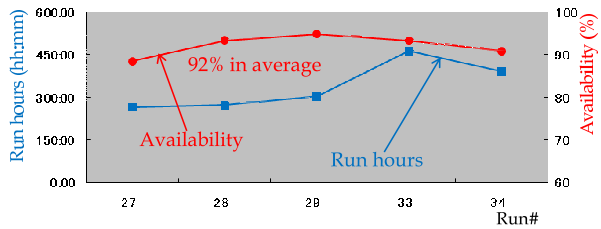

Figure 8: Beam availability for the MLF user operation in the last five run cycles.

and by introducing the beam loading compensation.

BEAM FAULT STATISTICS

Fig. 7-(a) and (b) shows beam fault statistics for the MLF user operation in the last five run cycles. The significant portion of the downtime related to the linac was from a fault of the RFQ and SDTL. The typical beam resuming time for the RFQ fault was 1 minute for automatic rf recovery case and 10 minutes for operator assisted recovery case. The failure rate of the automatic recovery, which mainly came from a severe discharge, was 20% in these cycles. The increase of the downtime related to the SDTL in the latest run cycle was from a discharge trouble of the coaxial feeder line. The downtime due to this incident reached to 7 hours. While this is a rare event, now we are monitoring temperatures at the feeder lines to get a sign. On the other hand, the downtime related to the RCS was mainly from a fault of the extraction kickers. In the RCS, eight sets of kicker magnets are installed and each magnet is operated by a power supply with two thyratrons. Since the thyratron is a gaseous discharge switching device, it often caused misfire or self-breakdown. As shown in Fig. 7-(b), the fault rate of the kickers is now significantly reduced by optimizing the reservoir voltage of thyratrons.

The total scheduled MLF user time in this period was

Table 1: Experimental conditions, where I_{peak}/L_{macro}/Chop show peak current/macro-pulse length/chopper beam-on duty factor of the injection beam, N_{bunch}/N_{part} are bunch number/particles per pulse, ϵ_{tp} is the transverse painting emittance, and V_{2nd}/$\Delta\phi$/Δp/p show amplitude of second harmonic rf voltage (ratio to the fundamental one)/phase sweep of second harmonic rf voltage relative to the fundamental one/momentum offset applied in the longitudinal painting.

Data ID	I_{peak} (mA)	L_{macro} (ms)	Chop (%)	N_{bunch}	N_{part}	Intensity (kW)	ϵ_{tp} (π mm mrad)	V_{2nd} (%)	$\Delta\phi$ (deg)	Δp/p (%)
(1)	15	0.1	56	2	5.0×10^{12}	60	-	-	-	-
(2)	15	0.2	56	2	1.0×10^{13}	120	-	-	-	-
(3)	15	0.3	56	2	1.5×10^{13}	180	-	-	-	-
(4)	15	0.4	56	2	2.0×10^{13}	240	-	-	-	-
(5)	15	0.5	56	2	2.5×10^{13}	300	-	-	-	-
(6)	15	0.5	56	2	2.5×10^{13}	300	100	-	-	-
(7)	15	0.5	56	2	2.5×10^{13}	300	100	80	-80	-
(8)	15	0.5	56	2	2.5×10^{13}	300	100	80	-80	-0.1
(9)	15	0.5	56	2	2.5×10^{13}	300	100	80	-80	-0.2

1696 hours, for which the beam availability defined as the beam-on time for MLF users/scheduled beam time promised to users was 92% (Fig. 8).

BEAM STUDY FOR FURTHER RAMPING UP THE OUTPUT BEAM POWER

In December 2009, we began on a parameter tuning for higher intensity beams ($\sim$300 kW) including a beam painting injection scheme at the RCS. The permissible range of intensity loss for 300 kW output operation with 181 MeV injection energy, which is determined by the current collimator capability of 4 kW, is 22% at the injection energy. On the other hand, the allowable intensity loss for 1 MW output operation with 400 MeV injection energy is 3% if assuming the same collimator limit at the injection energy. The above two operations give an equivalent space-charge detuning at each injection energy. Therefore, achieving 300 kW output with less than 3% intensity loss for 181 MeV injection energy is the first matter toward realizing 1 MW output with 400 MeV injection energy.

Fig. 9 shows beam survival rates in the RCS measured with a DC current transformer (DCCT) for different intensities and painting parameters (1)$\sim$(9) listed in Table 1. The intensity losses observed for (1)$\sim$(5) with no painting were 0.5$\sim$7% depending on the beam intensity only appearing around the injection energy. For a 300 kW-equivalent intensity beam causing $\sim$7% intensity loss, we performed the painting injection aiming at the beam loss reduction. As for the transverse painting [8], 100π mm mrad correlated painting was performed by sweeping the closed orbit in the horizontal plane and the injection orbit in the vertical plane. On the other hand, the longitudinal painting [9] was performed by the momentum-offset injection scheme (0$\sim-$0.2%) superposing a second harmonic rf voltage with an amplitude of 80% of the fundamental one. The phase sweep of the second harmonic rf voltage relative to the fundamental one ($-$80 to 0 degrees) was also employed so that the shape of the rf bucket was dynamically changed during the injection process. As shown in

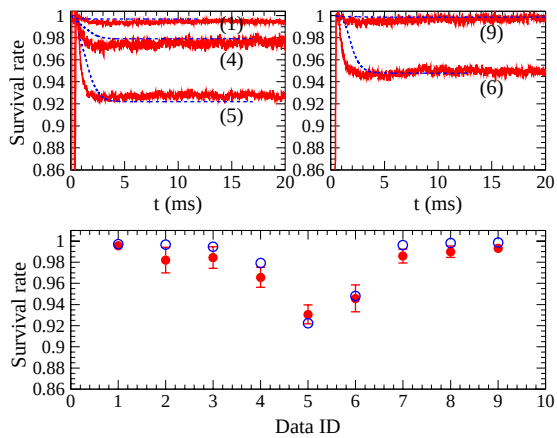

Figure 9: Beam survival rates measured with DCCT for different intensities and painting parameters listed in Table 1, where the blue dotted curves and blue circles are the results from the corresponding space-charge simulations. The quoted errors in the lower figure are pulse-by-pulse deviations in rms.

(6) and (9) of Fig. 9, the intensity loss was improved to $\sim$5% by the transverse painting, and finally minimized to $\sim$1% level by adding the longitudinal painting. In the figure, the blue dotted curves and blue circles are the results from the corresponding space-charge simulations including the following lattice imperfections; (A) scattering on the charge-exchange foil, (B) static leakage fields from the extraction beam line, (C) field and alignment errors, (D) edge focus of the injection-orbit bump magnets, and (E) multipole field components for all the ring magnets, where (B)$\sim$(E) are based on measurements. The calculated ones almost well reproduced the measured intensity losses for different intensities and painting parameters.

Fig. 10 shows incoherent tune spreads for the cases of (5) and (9) calculated at the end of the injection period. The current painting mitigates the space-charge detuning from ~-0.6 to ~-0.4. In order to understand the mechanism of the beam loss reduction by the current painting, we checked a time dependence of the beam moments obtained

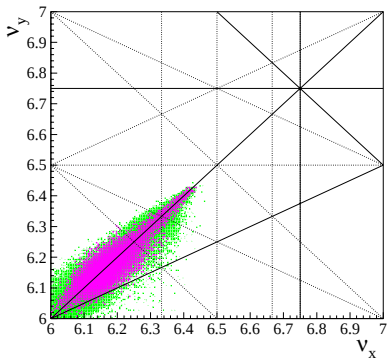

Figure 10: Incoherent tune shifts at the end of the injection, where the green one is calculated for (5) and the pink one is for (9).

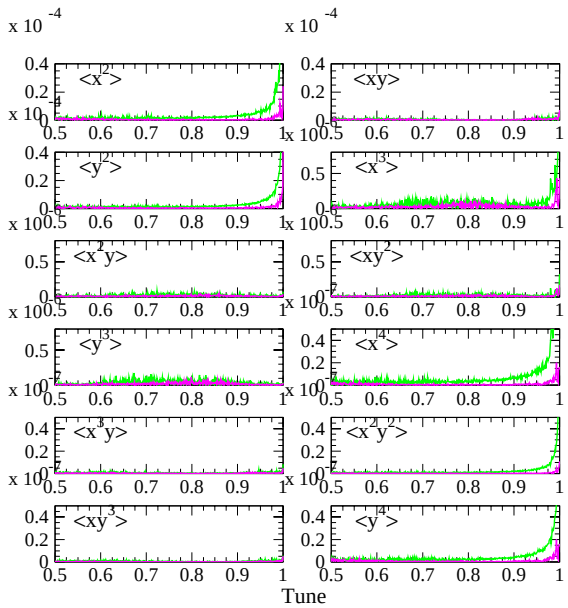

Figure 11: FFT spectra of the 2nd, 3rd and 4th-order coherent oscillations, where the green ones are calculated for (5), and the pink ones are for (9).

from the simulated transverse particle distributions. The influence of the resonance to the particle motion is reflected in the coherent oscillation of the corresponding beam moment; if the beam is captured in a resonance, the tune of the corresponding beam moment gets to integer. Fig. 11 shows FFT spectra of the 2nd, 3rd, and 4th-order coherent oscillations calculated for (5) and (9). While the spectra for $<x^2>$, $<y^2>$, $<x^3>$, $<x^4>$, $<x^2y^2>$ and $<y^4>$ have a significant peak at integer, they are significantly mitigated by the current painting. This analysis could say that the beam loss observed with no painting is mainly from the particles which satisfy the parametric resonance conditions at $\nu_{x,y}$=6, where various systematic resonances including high order can be excited. Fig. 12 shows normalized 99.9% emittances for (5) and (9) calculated with a systematic combination of the lattice imperfections (A)∼(E). In this calculation, the ring collimator aperture was not set to see the emittance growth in more detail. As shown in the figure, the emittance growth at the early stage of acceleration is significantly reduced by the painting. In introducing

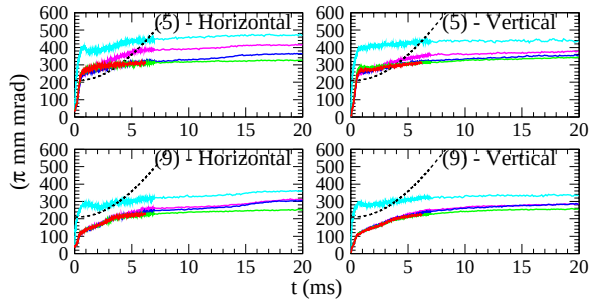

Figure 12: Normalized 99.9% emittances for (5) and (9) calculated with a systematic combination of the lattice imperfections; the light blue ones with all (A)∼(E), the pink ones with (B)∼(E), the blue ones with (C)∼(E), the green ones with (D)∼(E) and the red ones with only (E). The dotted black curves correspond to the ring collimator aperture of 324π mm mrad.

the painting, the events surpassing the collimator aperture is mainly from the emittance dilution caused by foil scattering. This means that the intensity loss for 300 kW beam is almost minimized by the painting injection.

SUMMARY

The linac and RCS started a user operation for the MLF in December 2008. The current output beam power to the MLF is 120 kW. Since December 2009, intensive studies for further ramping up the output beam power have been carried out, in which we successfully demonstrated a 300 kW output operation with a low intensity loss of 1% at the RCS by optimizing the painting injection. In this summer maintenance period, we have some measures for further beam loss reduction; vacuum improvement in the SDTL and future ACS section in the linac, and installation of AC power supplies for chromatic correction sextupoles and a small charge-exchange foil in the RCS. After completing such hardware improvements, we plan to increase the output beam power to 160 kW in December 2010, 200 kW in January 2011 and then 300 kW with carefully monitoring the trend of the machine activation.

REFERENCES

[1] JAERI-Tech 2003-044 and KEK Report 2002-13.

[2] M. Ikegami, Proc. of LINAC08, MO201 (2008).

[3] H. Hotchi *et al.*, Phys. Rev. ST Accel. Beams **12**, 040402 (2009).

[4] T. Koseki, in these proceedings (MOIB02).

[5] K. Yamamoto, in these proceedings (TU02C06).

[6] A. Miura *et al.*, Proc. of LINAC10, TUP075 (2010).

[7] H. Sako and M. Ikegami, Proc. of 2009 Annual Meeting of Particle Accelerator Society of Japan, p.217 (2009).

[8] P.K. Saha *et al.*, Phys. Rev. ST Accel. Beams **12**, 040403 (2009).

[9] F. Tamura *et al.*, Phys. Rev. ST Accel. Beams **12**, 041001 (2009).